2011

Temperature rise induced by a rotating or dithering laser beam

Zhou, Hong

Advanced Studies in Theoretical Physics / Volume 5, Issue 10, 443-468
https://hdl.handle.net/10945/25571

Adv. Studies Theor. Phys., Vol. 5, 2011, no. 10, 443 - 468

Temperature Rise induced by a Rotating or Dithering Laser Beam

Hong Zhou

Department of Applied Mathematics
Naval Postgraduate School
Monterey, CA 93943-5216, USA
hzhou@nps.edu

Abstract

We study the maximum temperature rise induced by a rotating or dithering Gaussian laser beam on a semi-infinite body. An analytical solution is obtained by solving the transient three-dimensional heat equation in a semi-infinite domain with insulating surface. The effect of rotating or dithering frequency on maximum temperature rise is quantitatively investigated for stainless steel and carbon nanotube-alumina composites. It is found that the maximum temperature rise can be reduced by increasing the frequency of the rotating or dithering beam and by increasing the radius of the rotating or dithering trajectory. For a fixed frequency, the maximum temperature rise induced by a rotating beam is lower than the one induced by a dithering beam. Finally, we give the asymptotic solution of the temperature rise for large frequency of a rotating Gaussian beam.

1 Introduction

Laser-induced heating has been widely applied in materials processing [17]. The theoretical modeling of temperature profiles induced by laser radiation in solids was pioneered by Lax [12, 13]. In [12] the spatial distribution of the temperature rise induced by a stationary Gaussian laser beam in a solid sample is modeled by a one-dimensional integral based on thermal conduction in the material. The integral is then evaluated numerically and it is found that the maximum temperature rise depends on the absorption depth of the laser energy. Since the closed-form solution in [12] is a steady state solution to the heat equation, it applies only for stationary or slow moving beams. The analysis of laser heating has been extended intensively to include temperature-dependent thermal conductivity[13, 14], time-dependent solution for a scanning Gaussian

beam [9], laser-melted front [4], continuous wave (cw) laser annealing of heterogeneous multilayer structures [8], temperature profiles induced by a moving cw elliptical laser beam with the inclusion of the temperature-dependent surface reflectivity and thermal diffusivity [15], a general analytic solution for the temperature rise produced by scanning Gaussian laser beams [19], the Green's function solution to the heat equation for a two-layer structure with scanning circular energy beams [6], the solution of the non-stationary heat equation with mixed boundary conditions using the Laplace transform and separation of variables method [1], analytical solution of the heat equation for moving semi-infinite medium under the effect of time dependent laser heat source [2], transient heat conduction in a thin metal film exposed to short-pulse laser heating using the dual phase lag heat conduction model, and laser short pulse heating with convective boundary condition [21]. Many of these studies are based on semi-infinite domains and quasi-steady states for a constant source speed. A transient, three-dimensional analytical solution of the temperature distribution in a finite solid when heated by a moving heat source is given in [3].

Recently laser forming of plates using a rotating or dithering beam is investigated [20]. However, to the best of our knowledge, a detailed study of the temperature rise induced by a rotating or dithering laser beam is not in the literature. For this reason, the present paper attempts to extend the work in [20] in order to investigate the effect of rotating or dithering speed of the laser beam on the maximum temperature rise. Our results will provide a quantative relationship between them and can be used to tune the speed of rotating or dithering beam in order to achieve a desirable temperature rise.

This paper is organized as follows. In Section 2 we review the mathematical modeling of the temperature distributions induced by a laser beam. We present our numerical results in Section 3 and derive the asymptotic solution in Section 4. Our main results are summarized in Section 5. Some mathematical details in Section 2 are shown in the Appendix.

2 Mathematical Formulation of the Problem

Consider a laser beam along the z direction, hitting a solid surface in the x-y plane and rotating in the x-y plane. This can be depicted schematically in Figure 1. A semi-infinite geometry is a reasonably good approximation if the laser beam is small compared to the object. In practice, the object surface can be made highly absorbing to the laser radiation by sand blasting and coating with collodial graphite. Heat loss from the target surface is assumed to be negligible compared to conduction into the solid. The mass density ρ, thermal conductivity K and specific heat C of the material are considered constant and evaluated at an average temperature.

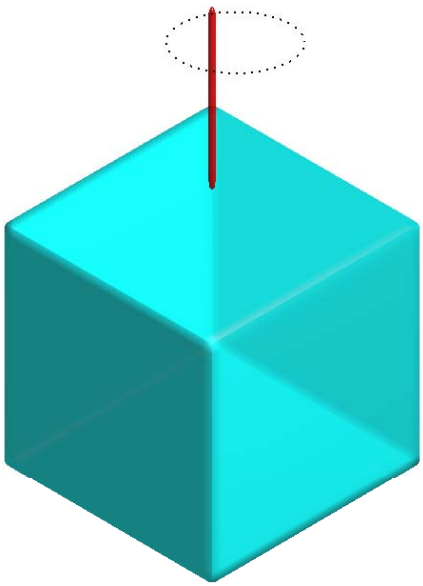

Figure 1: A schematic diagram shows a rotating laser beam shining on an object.

With all these assumptions, the governing equation is the transient three-dimensional heat conduction equation:

$$\frac{\partial T}{\partial t} = \alpha \Delta T + \frac{F(x, y, z, t)}{\rho\, C}, \tag{1}$$

where $T(x, y, z, t)$ is the solid's temperature rise above ambient (i.e. the difference between the object temperature and the ambient temperature) and it is a function of space and time, Δ is the Laplacian operator, $\alpha = \frac{K}{\rho\, C}$ is the thermal diffusivity, and the heat source term $F(x, y, z, t)$ is the energy distribution of the laser beam described above. We assume $F(x, y, z, t)$ has the form

$$F(x, y, z, t) \equiv f(x, y, t)\delta(z), \tag{2}$$

where the Dirac delta function $\delta(z)$ in z expresses the assumption that all the energy is absorbed at the surface.

Assume that the initial temperature rise is zero. When the boundary condition at $z = 0$ satisfies type 2 or Neumann condition (insulate), the solution

of the inhomogeneous heat equation (1) for a semi-infinite medium can be expressed as

$$T(x,y,z,t) = \frac{2\alpha}{K}\int_0^t \int_{R^2} \frac{f(x^{'},y^{'},s)}{[4\pi\alpha(t-s)]^{3/2}} \exp\left[-\frac{(x-x^{'})^2+(y-y^{'})^2+z^2}{4\alpha(t-s)}\right] dx^{'}dy^{'}ds, \tag{3}$$

where the three-dimensional Green's function has been used.

For a rotating Gaussian beam, the energy distribution of the laser beam $f(x,y,t)$ takes the form

$$f(x,y,t) = \frac{3Q}{\pi r_0^2}\exp\left[-\frac{(x-a\cos\frac{2\pi t}{s^*})^2+(y+b\sin\frac{2\pi t}{s^*})^2}{r_0^2/3}\right], \tag{4}$$

where Q is the power transferred into the substrate and it equals the product of the absorptivity and the laser power [20], r_0 is the characteristic beam radius typically defined as the radius at which the intensity of the laser beam drops to 5% of the maximum intensity, s^* is the rotating period and the parameters a and b are both positive. Note that (4) describes a clockwise rotating beam in the x-y plane. If $a = b$, then a denotes the radius of the rotation along the z-axis.

For a dithering Gaussian beam, $f(x,y,t)$ is given by

$$f(x,y,t) = \frac{3Q}{\pi r_0^2}\exp\left[-\frac{x^2+(y+c\sin\frac{2\pi t}{s^*})^2}{r_0^2/3}\right], \tag{5}$$

where $c > 0$ is the amplitude of every cycle.

Substituting the expression of f in (4) into the solution (3) yields the temperature rise induced by a rotating Gaussian beam:

$$\begin{aligned} T(x,y,z,t) = \frac{2\alpha Q}{K}\int_0^t \frac{1}{[4\pi\alpha(t-s)+\pi r_0^2/3]\sqrt{4\pi\alpha(t-s)}} \times \\ \exp\left[-\frac{z^2}{4\alpha(t-s)} - \frac{(x-a\cos\frac{2\pi s}{s^*})^2+(y+b\sin\frac{2\pi s}{s^*})^2}{4\alpha(t-s)+r_0^2/3}\right] ds. \end{aligned} \tag{6}$$

The detailed derivation of this formula is presented in the Appendix. The corresponding solution in the case of a dithering laser beam can be obtained from (6) by setting $a = 0$ and $b = c$.

To evaluate (6), we first make a change of variables in order to remove the singularity in the integrand:

$$u = \sqrt{4\alpha(t-s)},$$

and arrive at

$$T(x,y,z,t) = \frac{Q}{K}\int_0^{\sqrt{4\alpha t}} \frac{1}{\pi u^2 + \pi r_0^2/3} \times$$

$$\exp\left[-\frac{z^2}{u^2} - \frac{\left(x - a\cos\dfrac{2\pi t - \dfrac{\pi u^2}{2\alpha}}{s^*}\right)^2 + \left(y + b\sin\dfrac{2\pi t - \dfrac{\pi u^2}{2\alpha}}{s^*}\right)^2}{u^2 + r_0^2/3}\right] du. \tag{7}$$

The solution (7) can now be calculated by any numerical integration method, such as the composite Simpson's rule or Romberg integration method [5].

3 Numerical Results

We consider the temperature rise induced by rotating or dithering laser beams for two representative materials: stainless steel and carbon nanotube-alumina (CNT-Al_2O_3) nanocomposites.

Stainless steel is a group of iron-based metal containing at least 10% chromium (alloy metals). It plays an important role in our daily life with applications ranging from cookware to aviation products. The thermophysical properties of stainless steel are summarized in Table 1 [18].

	stainless steel	CNT-alumina
melting point (^oC)	1500	2040
density (kg/m^3)	7532	1340
specific heat (J/kg^oC)	629.5 (@ 1000^oC)	6090 (@ 400^oC)
thermal conductivity (W/m^oC)	27.07 (@ 1000^oC)	90.44 (@ 1550^oC)
thermal diffusivity (m^2/s)	5.709×10^{-6} (@ 1000^oC)	13.98×10^{-6} (@ 1550^oC)

For all the calculations presented in this paper, we choose the laser power as $500J/s$ or $500W$ and the absorptivity of the material is assumed to be 80%. The correpsonding value of Q is $400J/s$. The laser beam diameter is $4mm$. From the expression (7), it is obvious that the maximum temperature rise in the material occurs at the surface $z = 0$. Figure 2 gives several snapshots of

the temperature rise at $z = 0$ with $s^* = 0.05s$ at difference times. One can see from Figure 2 that the hottest spot is exactly where the laser beam hits the object. In Figure 3 we plot the temperature rise at $z = 0$ and $t = 1s$ for various values of rotating period s^* of the rotating laser beam. It is clear from Figure 3 that the maximum temperature rise decreases as the rotating period decreases. In other words, the slower the beam rotates, the hotter the object is. The quantitative relationship between the maximum temperature rise and the rotating frequency (i.e. reciprocal of the rotating period) at $t = 1s$ is depicted in Figure 4. Figure 5 shows the temperature rise as a function of time at a fixed point $(x, y, z) = (5, 0, 0)$ on the heated surface of the stainless steel material. The temperature rise oscillates and its envelope behaves as an increase function of time. In Figure 6 we compare the temperature rise at $z = 0$ for two different radii of rotating trajectory. Apparently, the temperature rise associated with larger radius of rotating trajectory ($a = 3mm$) is less than the one associated with smaller radius of rotating trajectory ($a = 2mm$). The dependence of maximum temperature rise on the radius of rotating trajectory is shown in Figure 7 which says that the maximum temperature rise is inversely proportional to the radius of rotating trajectory.

In Figures 8-13 we show the corresponding results of a dithering Gaussian beam on stainless steel. Similar results as above are observed for a dithering Gaussian beam: the maximum temperature rise is a decreasing function of the frequency of the dithering beam and the radius of dithering trajectory. Furthermore, comparing Figure 4 and Figure 10, one can see that for a fixed frequency, the maximum temperature rise induced by a rotating beam is lower than the one induced by a dithering beam.

Now we extend the above studies from stainless steel to carbon nanotube-Alumina nanocomposites which have been synthesized by direct growth of carbon nanotubes on alumina by chemical vapor deposition. CNT-alumina is a new generation of engineered CNT-ceramic materials with extremely improved thermal properties. The relevant thermophysical properties of CNT-alumina are listed in Table 1 [11]. It is clear from Table 1 that CNT-alumina has larger values of specific heat, thermal conductivity and thermal diffusivity than stainless steel. It is a better candidate if one wants a lower temperature rise.

The effect of rotating or dithering frequency of the Gaussin beam on the maximum temperature rise of CNT-Alumina is given in Figure 14. It is observed as before that larger frequency leads to lower maximum temperature rise. Eventually, the maximum temperature rise approaches an equilibrium value as frequency increases. The equilibrium value corresponding to the rotating Gaussian beam is smaller than that of the dithering Gaussin beam. Figure 15 describes the effect of laser beam radius on the maximum temperature rise. When the laser beam radius is smaller which corresponds to a more

focused beam, the maximum temperature rise becomes larger.

4 Asymptotic Behavior of the Temperature Rise for Large Frequency

In this section we investigate the asymptotic behavior of the temperature rise as the frequency of the rotating Gaussian beam goes to infinity.

Recall that the temperature rise due to a rotating Gaussian beam is given by 6. Since we are interested in the maximum temperature rise, we consider the case $z = 0$ and to facilitate our analysis, we assume $a = b$. Under these conditions, the expression of temperature rise becomes

$$T(x,y,0,t) = \frac{2\alpha Q}{K\pi^{\frac{3}{2}}} \int_0^t \frac{1}{[4\alpha(t-s)+r_0^2/3]\sqrt{4\alpha(t-s)}} \times \exp\left[-\frac{x^2+y^2+a^2-2a\sqrt{x^2+y^2}\cos(\frac{2\pi s}{s^*}+\theta_0)}{4\alpha(t-s)+r_0^2/3} \right] ds, \tag{8}$$

which θ_0 satisfies

$$\cos\theta_0 = \frac{x}{x^2+y^2}, \ \sin\theta_0 = \frac{y}{x^2+y^2}.$$

Using change of variables $s_{new} = \alpha(t-s)$ and then dropping the subscript, we write the temperature as

$$T(x,y,0,t) = \frac{2Q}{K\pi^{\frac{3}{2}}} \int_0^{\alpha t} \frac{1}{\sqrt{4s}h(s)} \times \exp\left[\frac{g_1(x,y)+g_2(x,y)\cos(\frac{2\pi s}{\epsilon}-\theta(t))}{h(s)} \right] ds, \tag{9}$$

where

$$\begin{aligned} &\epsilon = \alpha s^*, \ \ \theta(t) = \tfrac{2\pi t}{s^*} + \theta_0, \ \ h(s) = 4s + \tfrac{r_0^2}{3}, \\ &g_1(x,y) = -(x^2+y^2+a^2), \ \ g_2(x,y) = 2a\sqrt{x^2+y^2}. \end{aligned} \tag{10}$$

Our aim is to find a two-term asymptotic expansion for small ϵ (i.e. small period or large frequency of the rotating beam). To achieve this goal, we start by considering the Fourier expansion of $\exp(\eta\cos(u))$ as a function of u:

$$\exp(\eta\cos(u)) = \sum_{k=0}^{\infty} a_k(\eta)\cos(ku). \tag{11}$$

The Fourier expansion defines a sequence of coefficient functions $\{a_k(\eta),\ k = 0, 1, 2, \cdots\}$ which are given by

$$\begin{aligned} a_0(\eta) &= \tfrac{1}{2\pi}\int_0^{2\pi} \exp(\eta\cos(u))du, \\ a_k(\eta) &= \tfrac{1}{\pi}\int_0^{2\pi} \exp(\eta\cos(u))\cos(ku)du, \quad k = 1, 2, \cdots \end{aligned} \tag{12}$$

We remark that the Fourier expansion (11) is valid for any value of u and the Fourier coefficients (12) are one-dimensional functions which can be pre-calculated.

Using the Fourier expansion (11), we write the integrand function in (9) as

$$\text{integrand function} = \frac{1}{\sqrt{4s}h(s)} \exp\left[\frac{g_1(x,y)}{h(s)}\right] \sum_{k=0}^{\infty} a_k\left(\frac{g_2(x,y)}{h(s)}\right) \cos\left(k\frac{2\pi s}{\epsilon} - k\theta(t)\right).$$

Introduce the variable $s = u^2$ then the temperature can be expressed as

$$T(x, y, 0, t) = \frac{2Q}{K\pi^{3/2}} I_0 + \frac{2Q}{K\pi^{3/2}} \sum_{k=1}^{\infty} I_k, \tag{13}$$

where

$$\begin{aligned} I_0 &= \int_0^{\sqrt{\alpha t}} \frac{1}{h(u^2)} \exp\left[\frac{g_1(x,y)}{h(u^2)}\right] a_0\left(\frac{g_2(x,y)}{h(u^2)}\right) du, \\ I_k &= \int_0^{\sqrt{\alpha t}} \frac{1}{h(u^2)} \exp\left[\frac{g_1(x,y)}{h(u^2)}\right] a_k\left(\frac{g_2(x,y)}{h(u^2)}\right) \cos\left(k\frac{2\pi u^2}{\epsilon} - k\theta(t)\right) du,\ k > 0. \end{aligned} \tag{14}$$

Note that I_0 is the leading term. As we will show below, all other I_k (where $k > 0$) terms in the summation in (13) contribute to the second term in the asymptotic expansion.

We use the method of stationary phase to approximate I_k terms. The method of stationary phase is an asymptotic approximation technique which estimates integrals whose integrands rapidly oscillate in sign over the integration range. Due to oscillations, the contributions to the integral tend to cancel except at end points where small contributions remain. Contributions also arise from regions where the rate of oscillation of the integrand is reduced. Such regions are called regions of stationary phase. For a more detailed introduction to the method of stationary phase, see the excellent textbook by Bush [7]. We now turn to the evaluation of I_k. There is a single point of stationary phase occurring at $u = 0$. Applying the standard method of stationary phase, we find

$$I_k = \frac{1}{h(0)} \exp\left[\frac{g_1(x,y)}{h(0)}\right] a_k\left(\frac{g_2(x,y)}{h(0)}\right) \int_0^{\infty} \cos\left(k\frac{2\pi u^2}{\epsilon} - k\theta(t)\right) du + o(\sqrt{\epsilon}). \tag{15}$$

The integral requires results from Calculus, namely

$$\int_0^\infty \cos(\frac{2\pi k}{\epsilon}u^2)du = \int_0^\infty \sin(\frac{2\pi k}{\epsilon}u^2)du = \frac{1}{4\sqrt{k}}\sqrt{\epsilon} + o(\sqrt{\epsilon}). \tag{16}$$

Substituting the expressions (16) into (14) leads, after some manipulation, to the equation

$$\begin{aligned} I_k &= \frac{3}{r_0^2}\exp\left[\frac{3g_1(x,y)}{r_0^2}\right] a_k\left(\frac{3g_2(x,y)}{r_0^2}\right)[\cos(k\theta(t)) + \sin(k\theta(t))]\frac{1}{4\sqrt{k}}\sqrt{\epsilon} + o(\sqrt{\epsilon}) \\ &= \frac{3\sqrt{\epsilon}}{r_0^2 2\sqrt{2}\sqrt{k}}\exp\left[\frac{3g_1(x,y)}{r_0^2}\right] a_k\left(\frac{3g_2(x,y)}{r_0^2}\right)\cos(k\theta(t) - \frac{\pi}{4}) + o(\sqrt{\epsilon}). \end{aligned} \tag{17}$$

where we have used (10) to get $h(0) = r_0^2/3$.

Returning to (13), we have

$$\begin{aligned} T(x,y,0,t) &= \frac{2Q}{K\pi^{3/2}}\int_0^{\sqrt{\alpha t}} \frac{1}{h(u^2)}\exp\left[\frac{g_1(x,y)}{h(u^2)}\right] a_0\left(\frac{g_2(x,y)}{h(u^2)}\right) du \\ &+ \frac{6Q\sqrt{\epsilon}}{2\sqrt{2}K\pi^{3/2}r_0^2}\exp\left[\frac{3g_1(x,y)}{r_0^2}\right]\sum_{k=1}^{\infty}\frac{1}{\sqrt{k}}a_k\left(\frac{3g_2(x,y)}{r_0^2}\right)\cos(k\theta(t) - \frac{\pi}{4}) + o(\sqrt{\epsilon}). \end{aligned} \tag{18}$$

The first term on the right-hand side of this expression corresponds to the leading $O(1)$ term whereas the second term is of the order $O(\sqrt{\epsilon})$. Furthermore, $\theta(t) = 2\pi t/s^* + \theta_0$ gives the time dependence of the temperature rise. Numerical experiments show that the infinite sum in (18) converge very quickly so in numerical computations only a small number of terms are needed in approximating the sum.

The asymptotic result (18) predicts that the temperature behaves like $c_0 + c_1/\sqrt{\text{frequency}}$ for large frequency of the rotating beam where c_0 and c_1 are some constants. In Figure 16 we use the least square method to fit the curve in Figure 4 by a function $c_0 + c_1/\sqrt{\text{frequency}}$ where $c_0 = 577$ and $c_1 = 2698$. The excellent fitting in Figure 16 validates the asymptotic result.

5 Conclusions

In this paper we have given a quantative study on the temperature rise induced by a rotating or dithering Gaussian laser beam for stainless steel and CNT-alumina nanocomposites. The maximum temperature rise can be reduced by increasing the frequency of a rotating or dithering beam and by increasing the radius of the rotating or dithering trajectory. Furthermore, for a fixed frequency the maximum temperature rise induced by a rotating beam

is smaller than the one induced by a dithering beam.

Acknowledgment

We wish to thank the Office of Naval Research (ONR) for supporting this effort.

References

[1] N. Abdelrazaq, "The solution of heat conduction equation with mixed boundary conditions," Journal of Mathematics and Statistics 2 (2006) 346-350.

[2] R. T. Al-Khairy and Z. M. Al-Ofey, "Analytical solution of the hyperbolic heat conduction equation for moving semi-infinite medium under the effect of time-dependent laser heat source," Journal of Applied Mathematics 2009 (2009) Article ID 604695.

[3] G. Araya and G. Gutierrez, "Analytical solution for a transient, three-dimensional temperature distribution due to a moving laser beam," Int. J. Heat and Mass Transfer 49 (2006) 4124-4131.

[4] M. Bertolotti and C. Sibilia, "Depth and velocity of the laser-melted front from an anlytical solution of the heat conduction equation," IEEE J. Quantum Electron. QE-17 (1981) 1980-1989.

[5] R. L. Burden and J. D. Faires, *Numerical Analysis*, Thomson Brooks/Cole, eighth edition, 2005.

[6] M. L. Burgener and R. E. Reedy, "Temperature distributions produced in a two-layer structure by a scanning cw laser or electron beam," J. Appl. Phys. 53 (1982) 4357-4363.

[7] A. W. Bush, *Perturbation Methods for Engineers and Scientists*, CRC Press, Boca Raton, 1992.

[8] I. D. Calder and R. Sue, "Modeling of cw laser annealing of multilayer structures," J. Appl. Phys. 53 (1982) 7545-7550.

[9] H. E. Cline and T. R. Anthony, "Heat treating and melting material with a scanning laser or electron beam," J. Appl. Phys. 48 (1977) 3895-3900.

[10] F. John, *Partial Differential Equations*, Springer, New York, 1981.

[11] L. Kumari, T. Zhang, G.H. Du, W.Z. Li, Q.W. Wang, A. Datye and K.H. Wu, "Thermal properties of CNT-Alumina nanocomposites," Composites Science and Technology 68 (2008) 2178-2183.

[12] M. Lax, "Temperature rise induced by a laser beam," J. Appl. Phys. 48 (1977) 3919-3924.

[13] M. Lax, "Temperature rise induced by a laser beam II. The nonlinear case," Appl. Phys. Lett. 33(1978) 786-788.

[14] S. C. Mishra and T. B. Pavan Kumar, "Analysis of a hyperbolic heat conduction-radiation problem with temperature dependent thermal conductivity," Journal of Heat Transfer 131 (2009) 111302.

[15] J. E. Moody and R. H. Hendel, "Temperature profiles induced by a scanning cw laser beam," J. Appl. Phys. 53 (1982) 4364-4371.

[16] K. Ramadan, W. R. Tyfour and M. A. Al-Nimr, "On the analysis of short-pulse laser heating of metals using the dual phase lag heat conduction model," Journal of Heat Transfer 131 (2009) 111301.

[17] J. Ready, "Material Processing – An Overview," Proc. IEEE 70 (1982) 533-544.

[18] S. Rudtsch, *et al.*, "Intercomparison of thermophysical property measurements on an austenitic stainless steel," International Journal of Thermophysics 26 (2005) 855-867.

[19] D. J. Sanders, "Temperature distributions produced by scanning Gaussian laser beams," Applied Optics 23 (1984) 30-35.

[20] Me. Sistaninia, Ma. Sistaninia and H. Moeanodini, "Laser forming of plates using rotating and dithering beams," Computational Materials Science 45 (2009) 480-488.

[21] B. S. Yilbas, "Laser short pulse heating with convective boundary condition," Numerical Heat Transfer, Part A: Applications 38 (2010) 423-442.

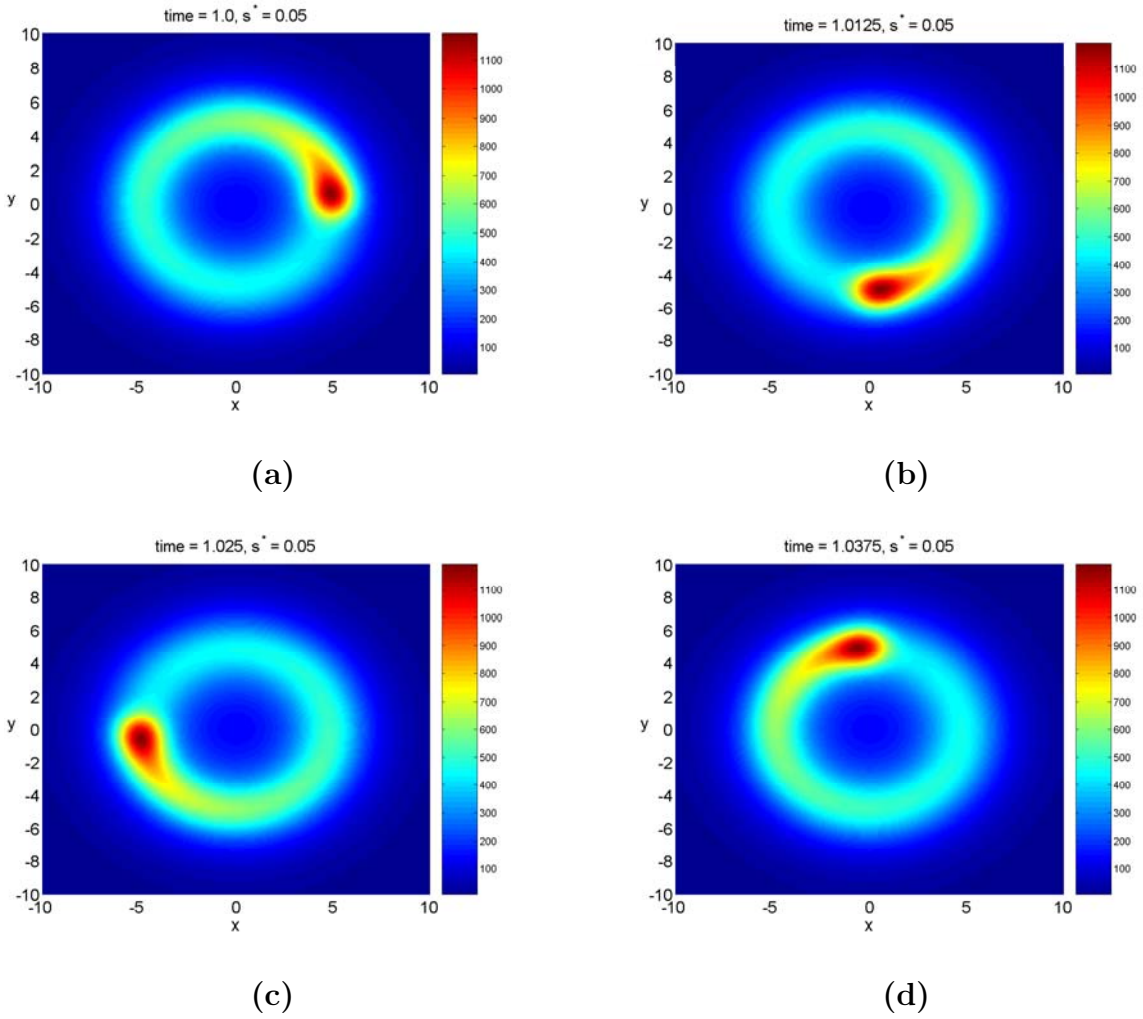

(a) **(b)**

(c) **(d)**

Figure 2: Snapshots of the temperature rise of stainless steel induced by a rotating Gaussian beam at the surface $z = 0$.

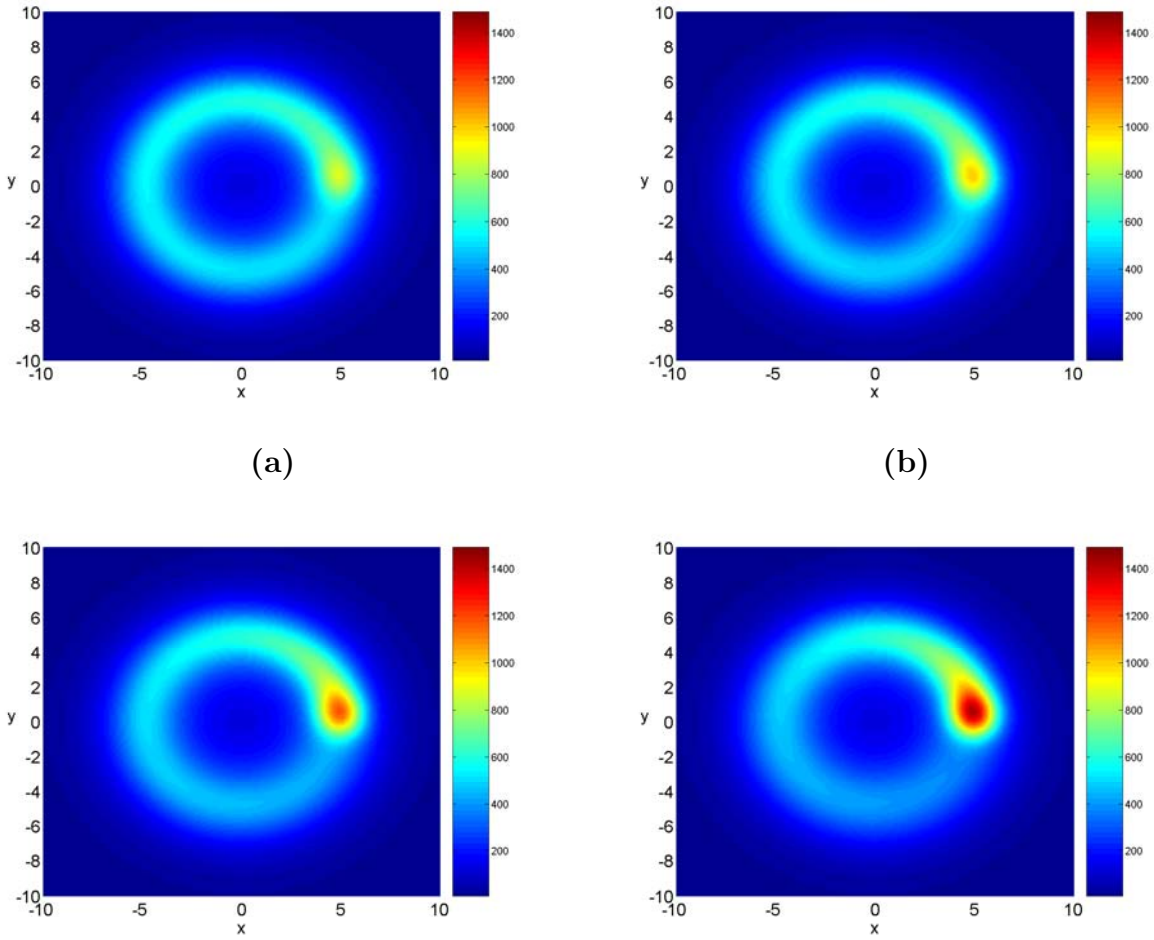

Figure 3: Temperature rise of stainless steel induced by a rotating Gaussian beam with different rotating period s^* at the surface $z = 0$: (a) $s^* = 0.0125s$; (b)$s^* = 0.025s$; (c) $s^* = 0.05s$; (d) $s^* = 0.1s$. Here the rotating radius is $a = b = 5mm$ and time $t = 1s$.

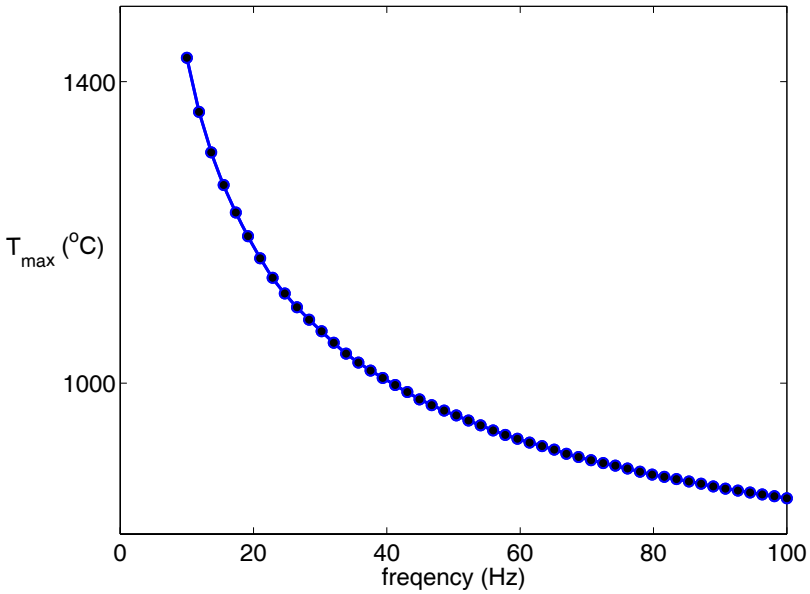

Figure 4: The maximum temperature rise of the stainless steel versus the frequency of the rotating Gaussian beam.

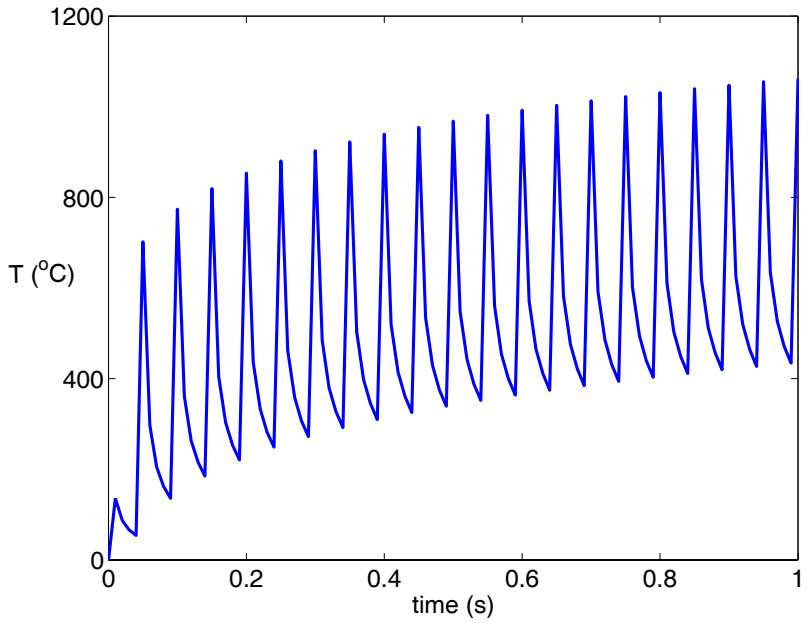

Figure 5: The temperature change with time at a fixed point $(x, y, z) = (5, 0, 0)$ on the material of stainless steel where the laser is a rotating Gaussian beam with period $s^* = 0.05s$.

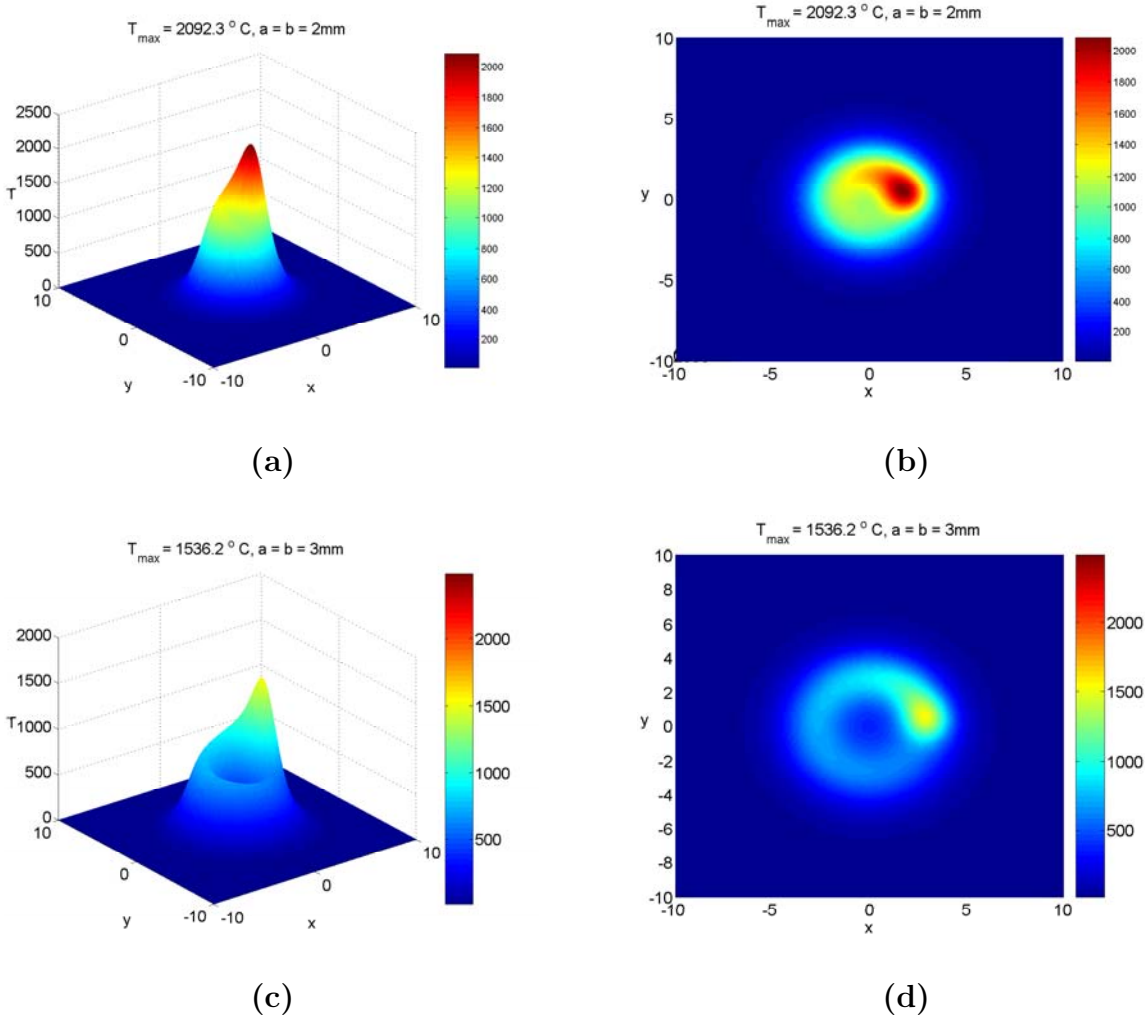

Figure 6: Temperature rise of stainless steel induced by a rotating Gaussian beam at time $t = 0.5s$ and $z = 0$ with different radius of rotating trajectory. Here $s^* = 0.05s$.

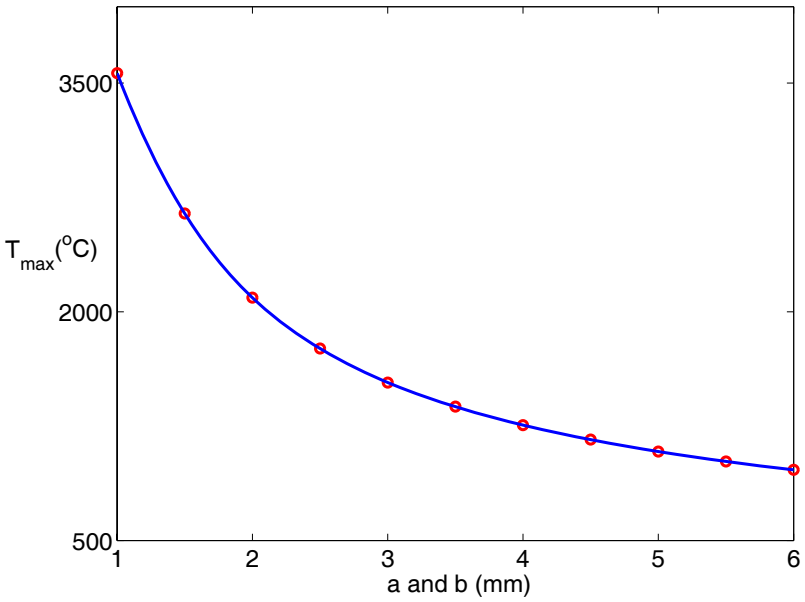

Figure 7: The maximum temperature rise versus the radius of rotating trajectory of the Gaussian beam. Here $a = b$, $t = 0.5s$ and $s^* = 0.05s$.

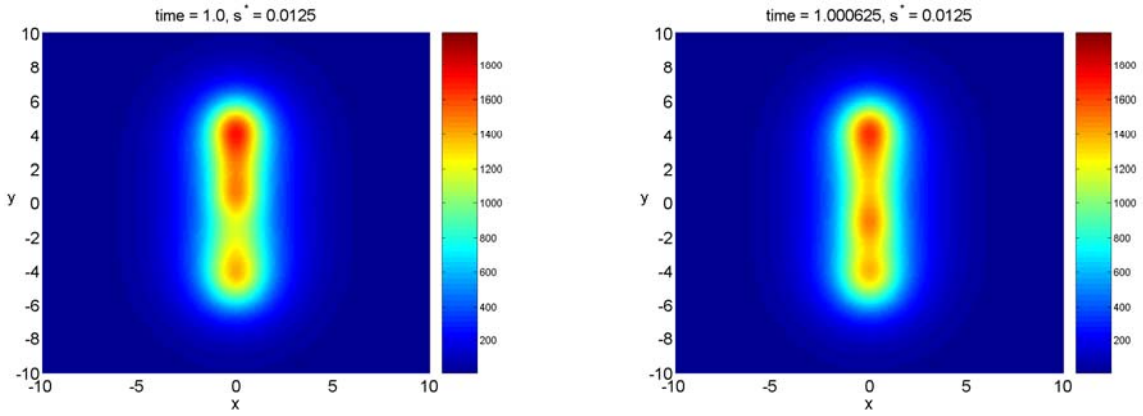

(a) **(b)**

(c) **(d)**

Figure 8: Snapshots of the temperature rise of stainless steel induced by a dithering Gaussian beam at the surface $z = 0$.

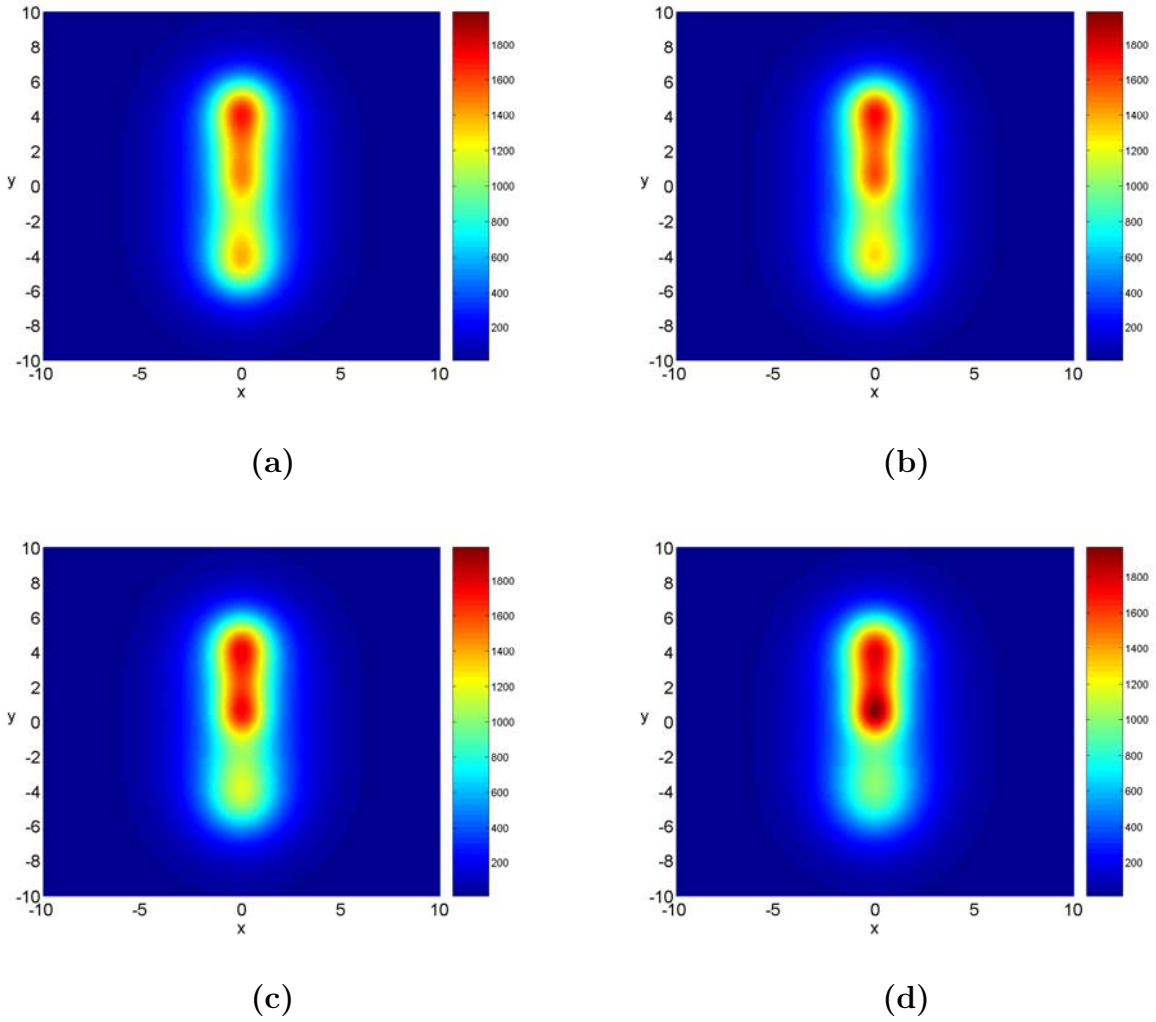

Figure 9: Temperature rise of stainless steel induced by a dithering Gaussian beam with different period s^* of each cycle at $z = 0$: (a) $s^* = 0.0125s$; (b)$s^* = 0.025s$; (c) $s^* = 0.05s$; (d) $s^* = 0.1s$. Here the amplitude of dithering is $c = 5mm$.

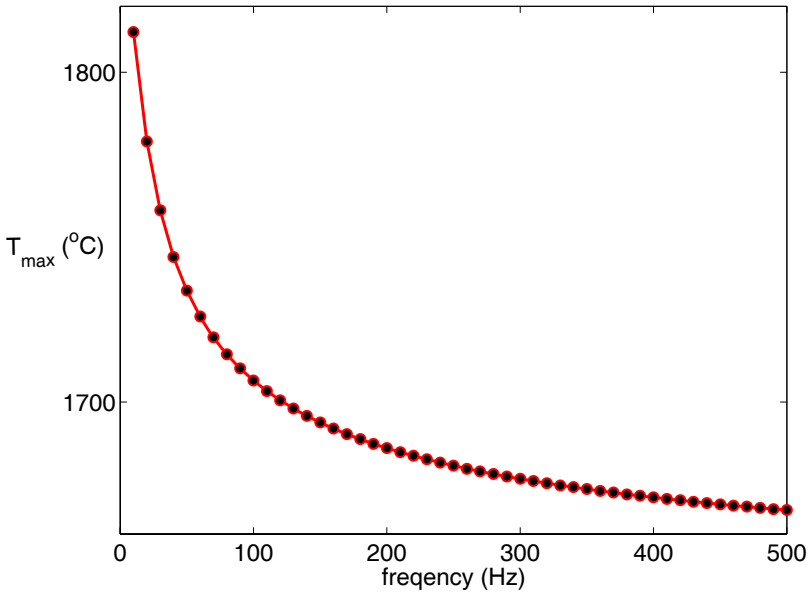

Figure 10: The maximum temperature rise of stainless steel versus the frequency of the dithering Gaussian beam.

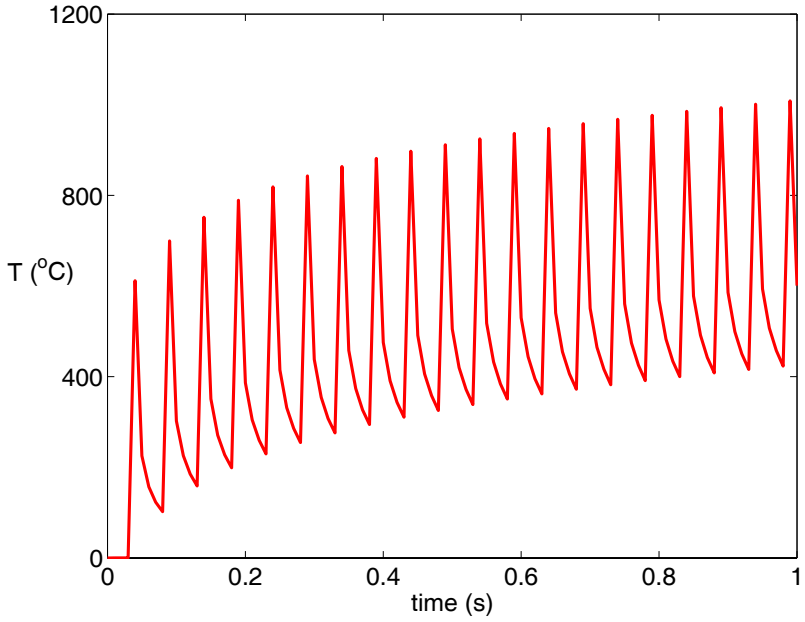

Figure 11: The temperature change with time at a fixed point $(x, y, z) = (0, 5, 0)$ on the material of stainless steel where the laser is a dithering Gaussian beam with period $s^* = 0.05s$.

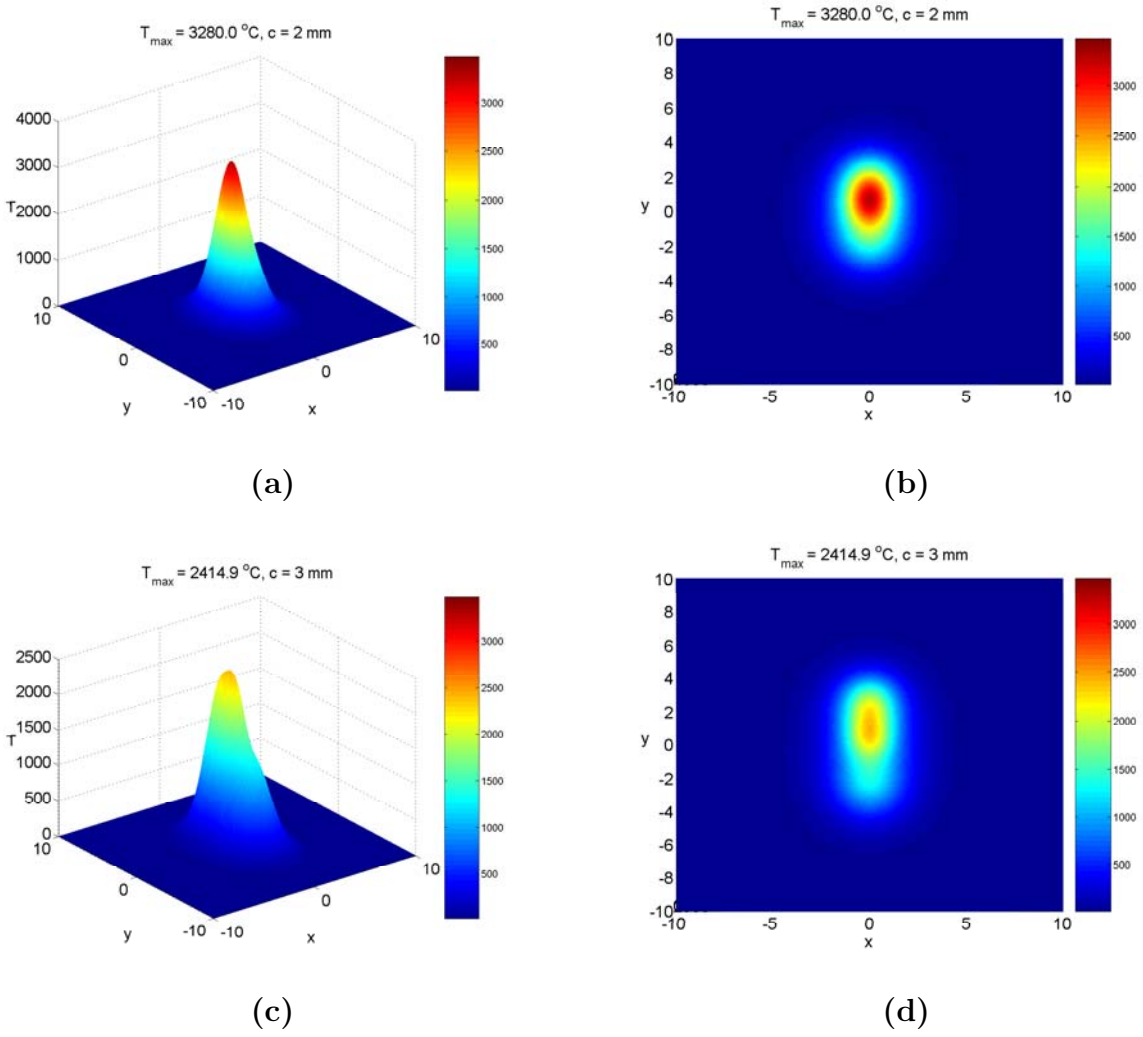

Figure 12: Temperature rise of stainless steel induced by a dithering Gaussian beam at time $t = 0.5s$ and $z = 0$ with different amplitude of dithering trajectory. Here $s^* = 0.05s$.

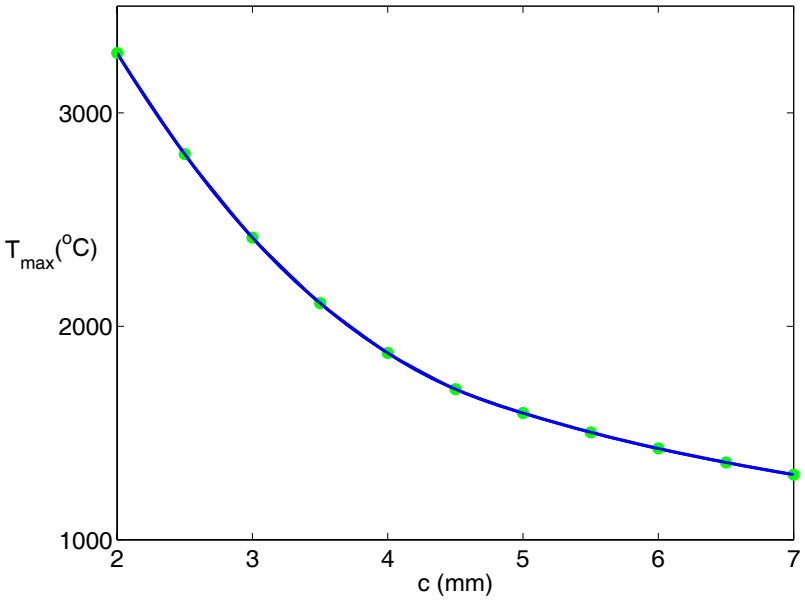

Figure 13: The maximum temperature rise versus the amplitude of dithering trajectory of the Gaussian beam. Here $t = 0.5s$ and $s^* = 0.05s$.

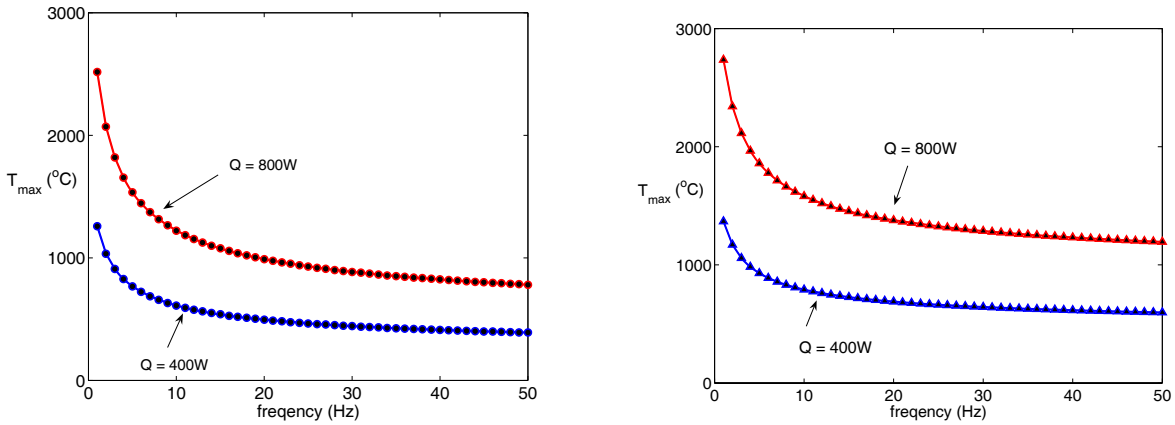

Figure 14: The maximum temperature rise of CTN-Alumina versus the frequency of the (a) rotating (b) dithering Gaussian beam with two different laser powers. Here $r_0 = 2mm$.

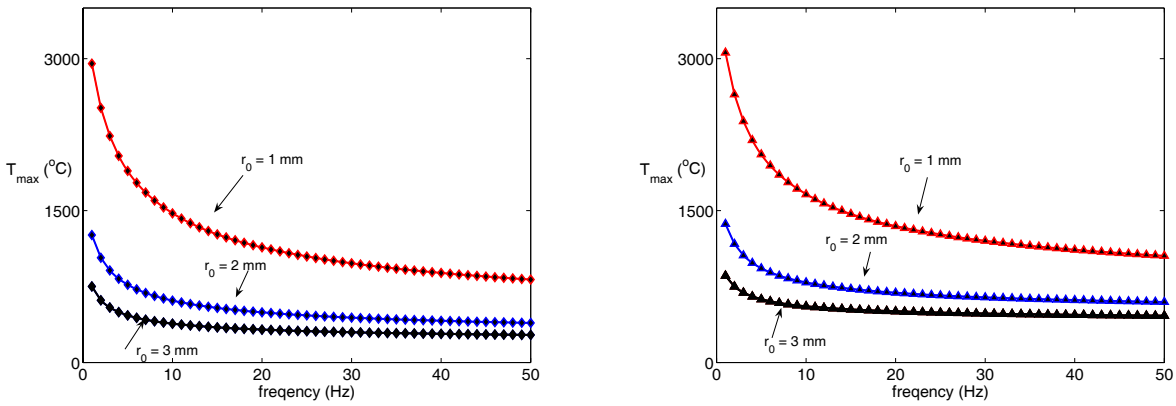

Figure 15: The maximum temperature rise of CTN-Alumina versus the frequency of the (a) rotating (b) dithering Gaussian beam with different beam radius. Here $Q = 400W$.

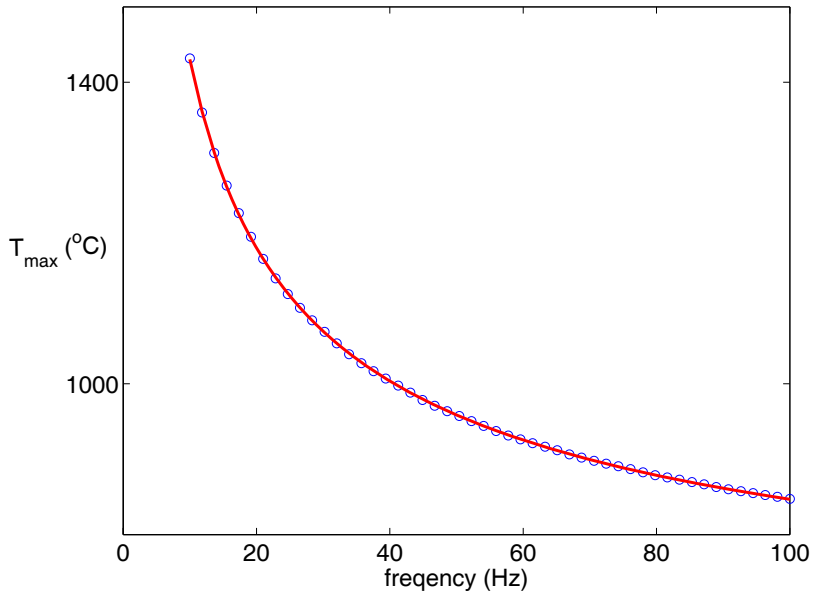

Figure 16: The numerical result from Figure 4 (dotted) vs the asymptotic prediction (solid line) given in Equation (18). Here the solid line is described by $T_{max} = 577 + 2698/\sqrt{\text{frequency}}$.

Appendix. Derivation of Formula (6)

In this appendix we give a simple derivation of formula (6).

For the reader's convenience, we recall that the general solution of the two-dimensional initial value problem

$$u_t = \alpha(u_{xx} + u_{yy}), \;\; u(x, y, 0) \text{ is known and } (x, y) \in R^2, \; t > 0 \tag{19}$$

is the convolution of the Green's function and the initial condition [10]:

$$u(x, y, t) = \int_{R^2} \left(\frac{1}{\sqrt{4\pi\alpha t}} \right)^2 \exp\left[-\frac{(x - x')^2 + (y - y')^2}{4\alpha t} \right] u(x', y', 0) dx' dy'. \tag{20}$$

Choose a special initial value $u(x, y, 0) = \delta(x - x_0, y - y_0)$ where δ is the Dirac delta function and (x_0, y_0) is a fixed arbitary point. Then the solution at time Δt becomes

$$u(x, y, \Delta t) = \frac{1}{4\pi\alpha\Delta t} \exp\left[-\frac{(x - x_0)^2 + (y - y_0)^2}{4\alpha\Delta t} \right]. \tag{21}$$

Now use $u(x, y, \Delta t)$ given in (21) as the initial value and go forward from time $= \Delta t$ to time $= t + \Delta t$. Then using (20) we have

$$\begin{aligned} u(x, y, t + \Delta t) = \int_{R^2} \frac{1}{4\pi\alpha t} \exp\left[-\frac{(x - x')^2 + (y - y')^2}{4\alpha t} \right] \times \\ \frac{1}{4\pi\alpha\Delta t} \exp\left[-\frac{(x' - x_0)^2 + (y' - y_0)^2}{4\alpha\Delta t} \right] dx' dy'. \end{aligned} \tag{22}$$

On the other hand, we know from (21) that

$$u(x, y, t + \Delta t) = \frac{1}{4\pi\alpha(t + \Delta t)} \exp\left[-\frac{(x - x_0)^2 + (y - y_0)^2}{4\alpha(t + \Delta t)} \right]. \tag{23}$$

It immediately follows from (22) and (23) that

$$\begin{aligned} &\int_{R^2} \frac{1}{4\pi\alpha t} \exp\left[-\frac{(x - x')^2 + (y - y')^2}{4\alpha t} \right] \exp\left[-\frac{(x' - x_0)^2 + (y' - y_0)^2}{4\alpha\Delta t} \right] dx' dy' \\ &= \frac{\Delta t}{t + \Delta t} \exp\left[-\frac{(x - x_0)^2 + (y - y_0)^2}{4\alpha(t + \Delta t)} \right]. \end{aligned} \tag{24}$$

Since Δt is arbitrary, one can denote $\sigma^2 \equiv \alpha \Delta t$. Then (24) is rewritten in the form

$$\int_{R^2} \frac{1}{4\pi\alpha t} \exp\left[-\frac{(x-x^{'})^2+(y-y^{'})^2}{4\alpha t}\right] \exp\left[-\frac{(x^{'}-x_0)^2+(y^{'}-y_0)^2}{4\sigma^2}\right] dx^{'}dy^{'}$$
$$= \frac{\sigma^2}{\alpha t+\sigma^2} \exp\left[-\frac{(x-x_0)^2+(y-y_0)^2}{4(\alpha t+\sigma^2)}\right]. \tag{25}$$

Now we consider the temperature rise induced by a rotating Gaussian beam. Combining (3) and (4), we find

$$T(x,y,z,t) = \frac{6\alpha Q}{\pi r_0^2 K} \int_0^t \int_{R^2} \frac{1}{[4\pi\alpha(t-s)]^{3/2}} \exp\left[-\frac{(x-x^{'})^2+(y-y^{'})^2+z^2}{4\alpha(t-s)}\right] \times$$
$$\exp\left[-\frac{(x^{'}-a\cos\frac{2\pi s}{s^*})^2+(y^{'}+b\sin\frac{2\pi s}{s^*})^2}{r_0^2/3}\right] dx^{'}dy^{'}ds$$
$$= \frac{6\alpha Q}{\pi r_0^2 K} \int_0^t \frac{1}{[4\pi\alpha(t-s)]^{3/2}} \exp\left[-\frac{z^2}{4\alpha(t-s)}\right]$$
$$\left\{\int_{R^2} \exp\left[-\frac{(x-x^{'})^2+(y-y^{'})^2}{4\alpha(t-s)}\right] \exp\left[-\frac{(x^{'}-a\cos\frac{2\pi s}{s^*})^2+(y^{'}+b\sin\frac{2\pi s}{s^*})^2}{r_0^2/3}\right]\right\} dx^{'}dy^{'}ds$$
$$= \frac{6\alpha Q}{\pi r_0^2 K} \int_0^t \frac{4\pi\alpha(t-s)}{[4\pi\alpha(t-s)]^{3/2}} \exp\left[-\frac{z^2}{4\alpha(t-s)}\right] \frac{r_0^2/12}{\alpha(t-s)+r_0^2/12} \times$$
$$\exp\left[-\frac{(x-a\cos\frac{2\pi s}{s^*})^2+(y+b\sin\frac{2\pi s}{s^*})^2}{4\alpha(t-s)+r_0^2/3}\right], \tag{26}$$

where in the last step the double integral is evaluated by using (25). After some straightforward algebra, (26) is simplified to:

$$T(x,y,z,t) = \frac{2\alpha Q}{K} \int_0^t \frac{1}{[4\pi\alpha(t-s)+\pi r_0^2/3]\sqrt{4\pi\alpha(t-s)}} \times$$
$$\exp\left[-\frac{z^2}{4\alpha(t-s)} - \frac{(x-a\cos\frac{2\pi s}{s^*})^2+(y+b\sin\frac{2\pi s}{s^*})^2}{4\alpha(t-s)+r_0^2/3}\right] ds, \tag{27}$$

which is exactly formula (6).

Received: October, 2010